Silicon-waveguide-coupled high-Q chalcogenide microspheres

Daniel H. Broaddus,[1,*] Mark A. Foster,[1] Imad H. Agha,[1,2] Jacob T. Robinson,[3] Michal Lipson,[3] and Alexander L. Gaeta,[1]

[1]*School of Applied and Engineering Physics, Cornell University, Ithaca, NY 14853, USA*
[2]*Currently with the Laboratorie de Charles Fabry de l'Institut de Optique, CNRS, Université Paris-sud, Campus Polytechnique, RD 128, 91127 Palaiseau cedex, France*
[3]*School of Electrical and Computer Engineering, Cornell University, Ithaca, NY, 14853, USA*
[*]*Corresponding author: dhb29@cornell.edu*

Abstract: We fabricate high-Q arsenic triselenide glass microspheres through a three-step resistive heating process. We demonstrate quality factors greater than 2×10^6 at 1550 nm and achieve efficient coupling via a novel scheme utilizing index-engineered unclad silicon nanowires. We find that at powers above 1 mW the microspheres exhibit high thermal instability, which limits their application for resonator-enhanced nonlinear optical processes.

OCIS codes: (220.4000) Microstructure fabrication; (160.2750) Glass and other amorphous materials; (230.5750) Resonators.

References and links

1. K. J. Vahala, "Optical microcavities," Nature **424,** 839-846 (2003).
2. I. H. Agha, J. E. Sharping, M. A. Foster, and A. L. Gaeta, "Optimal sizes of silica microspheres for linear and nonlinear optical interactions," Appl. Phys. B **83,** 303-309 (2006).
3. M. Gorodetsky and V. Ilchenko, "Optical microsphere resonators: Optimal coupling to high-Q whispering-gallery modes," J. Opt. Soc. Am. B **16,** 147-154 (1999).
4. D. Vernooy, V. Ilchenko, H. Mabuchi, E. Streed, and H. Kimble, "High-Q measurements of fused-silica microspheres in the near infrared," Opt. Lett. **23,** 247-249 (1998).
5. B. Little, J. Laine, and H. Haus, "Analytic theory of coupling from tapered fibers and half-blocks into microsphere resonators," J. Lightwave Technol. **17,** 704-715 (1999).
6. M. Cai, O. Painter, and K. J. Vahala, "Observation of critical coupling in a fiber taper to a silica-microsphere whispering-gallery mode system," Phys. Rev. Lett. **85,** 74-77 (2000).
7. T. Kippenberg, S. Spillane, D. Armani, and K. Vahala, "Ultralow-threshold microcavity raman laser on a microelectronic chip," Opt. Lett. **29,** 1224-1226 (2004).
8. T. J. Kippenberg, S. M. Spillane, and K. J. Vahala, "Kerr-nonlinearity optical parametric oscillation in an ultrahigh-Q toroid microcavity," Phys. Rev. Lett. **93,** 083904 (2004).
9. S. M. Spillane, T. J. Kippenberg, and K. J. Vahala, "Ultralow-threshold raman laser using a spherical dielectric microcavity," Nature **415,** 621-623 (2002).
10. I. H. Agha, Y. Okawachi, M. A. Foster, J. E. Sharping, and A. L. Gaeta, "Four-wave-mixing parametric oscillations in dispersion-compensated high-Q silica microspheres," Phys. Rev. A **76,** 043837-4 (2007).
11. P. Del'Haye, A. Schliesser, O. Arcizet, T. Wilken, R. Holzwarth, and T. J. Kippenberg, "Optical frequency comb generation from a monolithic microresonator," Nature **450,** 1214-1217 (2007).
12. A. Hilton, "Optical properties of chalcogenide glass," J. Non-Cryst. Solids **2,** 28-39 (1970).
13. J. S. Sanghera, L. B. Shaw, L. E. Busse, V. Q. Nguyen, P. C. Pureza, B. C. Cole, B. B. Harrison, I. D. Aggarwal, R. Mossadegh, F. Kung, D. Talley, D. Roselle, and R. Miklos, "Development and infrared applications of chalcogenide glass optical fibers," Fiber Integr. Opt. **19,** 251-274 (2000).
14. B. J. Eggleton, V. G. Ta'eed, and B. Luther-Davies, "Chalcogenide glass advanced for all-optical processing," Photonics Spectra **41,** (2007). http://www.photonics.com/content/spectra/2007/September/features/88885.aspx.
15. V. Ta'eed, N. Baker, L. Fu, K. Finsterbusch, M. Lamont, D. Moss, H. Nguyen, B. Eggleton, D. Choi, S. Madden, and B. Luther-Davies, "Ultrafast all-optical chalcogenide glass photonic circuits," Opt. Express **15,** 9205-9221 (2007).
16. M. Asobe, H. Itoh, T. Miyazawa, and T. Kanamori, "Efficient and ultrafast all-optical switching using high Δn, small core chalcogenide glass fibre," Electron. Lett. **29,** 1966-1968 (1993).

#107493 - $15.00 USD Received 11 Feb 2009; revised 23 Mar 2009; accepted 25 Mar 2009; published 30 Mar 2009

17. V. Ta'eed, L. Fu, M. Pelusi, M. Rochette, I. Littler, D. Moss, and B. Eggleton, "Error free all optical wavelength conversion in highly nonlinear As-Se chalcogenide glass fiber," Opt. Express **14,** 10371-10376 (2006).
18. L. Fu, M. Rochette, V. Ta'eed, D. Moss, and B. Eggleton, "Investigation of self-phase modulation based optical regeneration in single mode As_2Se_3 chalcogenide glass fiber," Opt. Express **13,** 7637-7644 (2005).
19. R. E. Slusher, G. Lenz, J. Hodelin, J. Sanghera, L. B. Shaw, and I. D. Aggarwal, "Large raman gain and nonlinear phase shifts in high-purity As_2Se_3 chalcogenide fibers," J. Opt. Soc. Am. B **21,** 1146-1155 (2004).
20. O. Kulkarni, C. Xia, D. Lee, M. Kumar, A. Kuditcher, M. Islam, F. Terry, M. Freeman, B. Aitken, S. Currie, J. McCarthy, M. Powley, and D. Nolan, "Third order cascaded Raman wavelength shifting in chalcogenide fibers and determination of Raman gain coefficient," Opt. Express **14,** 7924-7930 (2006).
21. E. C. Magi, L. B. Fu, H. C. Nguyen, M. R. Lamont, D. I. Yeom, and B. J. Eggleton, "Enhanced kerr nonlinearity in sub-wavelength diameter As_2Se_3 chalcogenide fiber tapers," Opt. Express **15,** 10324-10329 (2007).
22. L. Fu, A. Fuerbach, I. Littler, and B. Eggleton, "Efficient optical pulse compression using chalcogenide single-mode fibers," Appl. Phys. Lett. **88,** (2006).
23. A. Husakou and J. Herrmann, "Supercontinuum generation in photonic crystal fibers made from highly nonlinear glasses," Appl. Phys. B **77,** 227-234 (2003).
24. D. Yoem, E. Magi, M. Lamont, M. Roelens, L. Fu, and B. J. Eggleton, "Low-threshold supercontinuum generation in highly nonlinear chalcogenide nanowires," Opt. Lett. **33,** 660-662 (2008).
25. V. Ta'eed, M. Shokooh-Saremi, L. Fu, D. Moss, M. Rochette, I. Littler, B. Eggleton, Y. Ruan, and B. Luther-Davies, "Integrated all-optical pulse regenerator in chalcogenide waveguides," Opt. Lett. **30,** 2900-2902 (2005).
26. N. D. Psaila, R. R. Thomson, H. T. Bookey, S. Shen, N. Chiodo, R. Osellame, G. Cerullo, A. Jha, and A. K. Kar, "Supercontinuum generation in an ultrafast laser-inscribed chalcogenide glass waveguide," Opt. Express **15,** 15776-15781 (2007).
27. G. Boudebs, S. Cherukulappurath, M. Guignard, J. Troles, F. Smektala, and F. Sanchez, "Linear optical characterization of chalcogenide glasses," Opt. Commun. **230,** 331-336 (2004).
28. G. R. Elliott, D. W. Hewak, G. S. Murugan, and J. S. Wilkinson, "Chalcogenide glass microspheres; their production, characterization and potential," Opt. Express **15,** 17542-17553 (2007).
29. Y. Ruan, M. Kim, Y. Lee, B. Luther-Davies, and A. Rode, "Fabrication of high-Q chalcogenide photonic crystal resonators by e-beam lithography," Appl. Phys. Lett. **90,** 071102-3 (2007).
30. J. Hu, N. Carlie, L. Petit, A. Agarwal, K. Richardson, and L. Kimerling, "Demonstration of chalcogenide glass racetrack micro-resonators," Opt. Lett. **33,** 761-763 (2008).
31. C. Grillet, S. Bian, E. Magi, and B. Eggleton, "Fiber taper coupling to chalcogenide microsphere modes," Appl. Phys. Lett. **92,** 171109 (2008).
32. J. Hu, N. Carlie, N. Feng, L. Petit, A. Agarwal, K. Richardson, and L. Kimerling, "Planar waveguide-coupled, high-index-contrast, high-Q resonators in chalcogenide glass for sensing," Opt. Lett. **33,** 2500-2502 (2008).
33. A. Snyder and J. Love, *Optical Waveguide Theory*, (Kluwer Academic Publishers, 1983).
34. V. Almeida, R. Panepucci, and M. Lipson, "Nanotaper for compact mode conversion," Opt. Lett. **28,** 1302-1304 (2003).
35. V. Almeida, C. Barrios, R. Panepucci, and M. Lipson, "All-optical control of light on a silicon chip," Nature **431,** 1081-1084 (2004).
36. H. Naito, H. Amii, M. Okuda, and T. Matsushita, "Structural changes in amorphous arsenic triselenide below the glass-transition temperature," J. Non-Cryst. Solids **164-166,** 1239-1242 (1993).
37. E. D. Black, "An introduction to Pound-Drever-Hall laser frequency stabilization," Am. J. Phys. **69,** 79-87 (2001).

1. Introduction

The investigation of high quality factor (Q) cavities has grown into a mature research field, with fabrication techniques and applications seeing great refinements in the past several years [1-11]. Recently, work has leveraged the field buildup in small mode volume V, high-Q resonators to explore ultra-low threshold nonlinear optics (NLO). The figure of merit (FOM) for nonlinear interactions in such microcavities is Q^2/V, and Raman oscillation and four-wave mixing (FWM) were demonstrated in both silica microtoroids [7,8] and silica microspheres at low powers [9,10].

Initially explored for their high transmission in the near-IR and mid-IR [12,13], chalcogenide glasses have recently attracted significant interest as a material for NLO [14,15]. Chalcogenides exhibit large refractive indices, large nonlinear refractive indices n_2, and large Raman gain coefficients. The combination of high waveguiding confinement, achieved through high index contrast with silica and air and large n_2 allows for the fabrication of extremely compact fiber [16-23] and on-chip devices [24-26]. Applications such as all-optical switching [16], wavelength conversion [17], signal regeneration [18,25], Raman gain [19,20],

#107493 - $15.00 USD Received 11 Feb 2009; revised 23 Mar 2009; accepted 25 Mar 2009; published 30 Mar 2009

super-continuum generation [23,24,26], and pulse compression have already been demonstrated in chalcogenide waveguides. Arsenic triselenide (As_2Se_3), a chalcogenide glass, exhibits a particularly large nonlinear refractive index of $n_2 = 2.4\times10^{13}$ cm^2/W and a large Raman gain coefficient of 5.1×10^{-9} cm/W, which is 930× and 780×, respectively, that of silica glass [19]. It also exhibits a wide transmission window extending from 1 μm to 17 μm [13]. In addition, As_2Se_3 has a large refractive index of 2.83 and an absorption of 5 m^{-1} at 1550 nm [27].

Recently, chalcogenide glass microresonators have been demonstated [28-32]. When paired with the Q^2/V resonator enhancement for NLO interactions, As_2Se_3 offers promise for low-power NLO, particluarly in the NIR and MIR regime. Typically, silica microspheres have Q's exceeding 10^8 [9,10], while those of chalcogenide glass microresonators are ~10^5 [28-32]. Therefore, to be competive with silica, further refinement of chalcogenide microresonator systems is necessary.

Here we fabricate high-Q As_2Se_3 microspheres and overcome phase matching challenges by coupling to the microspheres with index-tailored silicon nanowires. We demonstrate a $Q > 2\times10^6$, which to our knowledge is the highest Q achieved in a chalcogenide microresonator. We also explore thermal instabilites in these microspheres and show that these instablilites are present at incident laser powers of 1 mW. Ultimately, these instabilities will limit the viability of As_2Se_3 as a material for nonlinear-optical microresonators.

2. Theory

High-Q resonator systems require a means of coupling light into the cavity. For optimal buildup in the resonator cavity, the interaction between the cavity and the coupling mechanism must be accurately controlled. Evanescent coupling from a fiber taper has been shown to provide sufficient degrees of freedom to achieve critical coupling to silica microspheres [5,6]. Futhermore, waveguide coupler geometries such as fiber tapers offer ease of integration with external systems.

Controlling phase matching in waveguide coupling schemes is a key parameter for achieving efficient coupling into the high index chalcogenide microspheres. The propagation constant mismatch $\Delta\beta$ between the waveguide and the microsphere mode is

$$\Delta\beta = \frac{\omega}{c}(n_s - n_w), \tag{1}$$

where n_s is the effective index of the sphere mode, and n_w is the effective index of the waveguide mode. Coupling efficiency falls off exponentially with the square of $\Delta\beta$ [5]. Figure 1(a) shows the effective index of the fundamental mode versus the sphere diameter for As_sSe_3 microspheres, and Fig. 1(b) shows the effective index of both silica and silicon waveguides versus the material index multiplied by the cross sectional area.

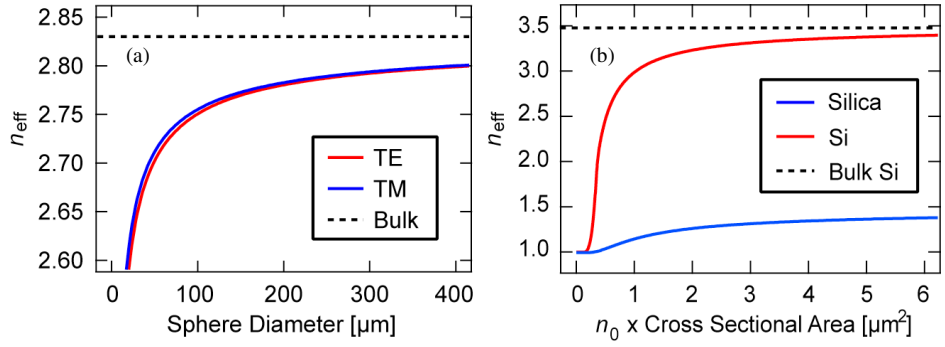

Fig. 1. Effective indices of As_2Se_3 microspheres, silicon nanowires, and silica nanowires. (a) Effective index vs. sphere diameter for fundamental TE (red) and TM (blue) modes in an As_2Se_3 microsphere. (b) Effective index vs. material index multiplied by cross sectional area of silicon (red) and silica (blue) waveguides.

#107493 - $15.00 USD Received 11 Feb 2009; revised 23 Mar 2009; accepted 25 Mar 2009; published 30 Mar 2009

Appropriate phase matching can only be achieved via a waveguide with equal or greater material index than the microsphere's effective index, since the effective index of a guided mode is always less than that of the material index of the core for waveguides based on total internal reflection [33]. Our simulations show that silicon nanowaveguides with a cross sectional area less than 0.3 μm^2 can achieve phase matching with such microspheres. These waveguides offer a robust coupling platform, a convenient waveguide coupling geometry, and easy integration into both on-chip and fiber systems [34,35].

3. Fabrication

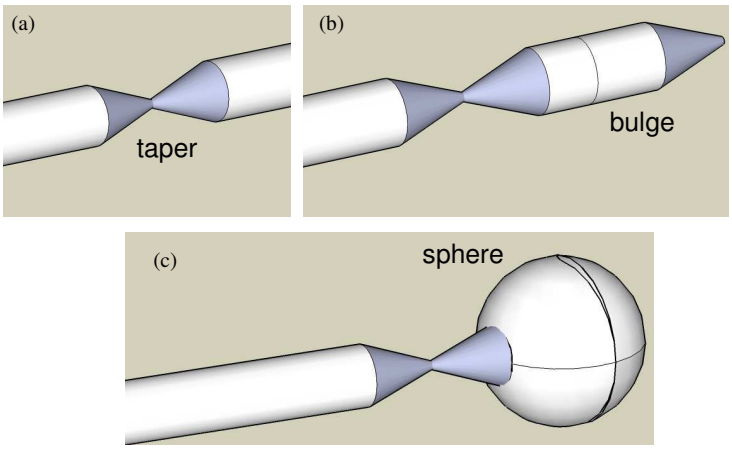

Fig. 2. Mockup of the three-step sphere fabrication process. (a) Taper with 15-μm waist. (b) Bulge formed by cinching off end of fiber. (c) Sphere formed using surface tension of molten As_xSe_3.

We fabricate the high-Q As_2Se_3 microspheres using resistive heating and a three-step process. We utilize a platinum heater, which allows for fabrication under normal lab conditions, including humidity and O_2 concentration. Oxidation on the surface of the sphere may contribute to overall loss; however, the effects were not investigated in this paper. Using this process, we fabricate microspheres with high surface quality over a size range of 55-400 μm. We begin with IRT-SE-06-01 As_2Se_3 step-index fiber available commerically from CorActive. We then taper the fiber down to a waist size of 15 μm with a sharp transition. We taper at a temperature of 200°C, which is slightly above the glass transition temperature (177°C) [36], and then translate 400-1200 μm along the fiber axis and taper until we cinch off the end of the fiber, which leaves a bulge. We control the size of the bulge by changing the distance translated, which determines the volume of the sphere. We then heat the bulge above the melting point (320°C) of the chalcogenide glass, and the surface tension of the molten chalcogenide glass molds the bulge into a spherical shape. Due to the rotational symmetry of the fiber and fabrication process the microspheres have low on-axis eccentricity. Figure 2 shows a mockup of the three steps, and Fig. 3 shows three completed spheres.

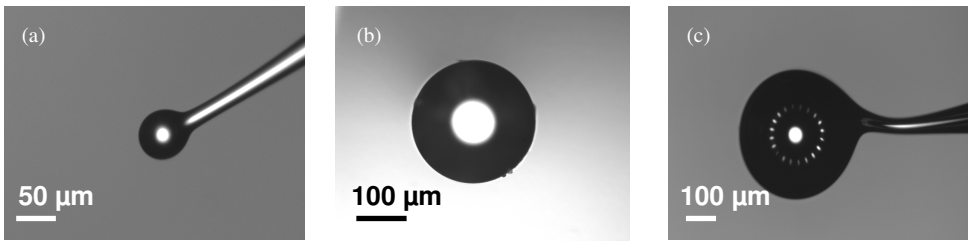

Fig. 3. Three completed microspheres showing good surface quality and diameters of (a) 55 μm, (b) 270 μm (on fiber axis e = 0.086), and (c) 384 μm.

#107493 - $15.00 USD Received 11 Feb 2009; revised 23 Mar 2009; accepted 25 Mar 2009; published 30 Mar 2009

4. Experiment

Figure 4 shows a schematic of our coupling and detection scheme. To characterize the microspheres, light from an external-cavity diode laser is coupled into the sphere, and the frequency is repeatedly tuned over several GHz via piezo control. An erbium-doped fiber amplifier (EDFA) amplifies the signal, which is then coupled into an unclad silicon rib waveguide via a tapered lens fiber. The waveguides have cross sectional dimensions of 900 nm by 250 nm and are fabricated on a SiO_2 substrate. At the point of coupling to the microsphere, the waveguides taper down to a cross section of 250 nm by 250 nm. This corresponds to n_{eff} ranging from 2.9 to 1.1 in the waveguides. We control coupling to the microsphere by bringing the microsphere in contact with the photonic chip and translate it transversely to the waveguide over the tapered region until optimal coupling is achieved. We then detect the output signal with a photodiode and view its output on an oscilloscope.

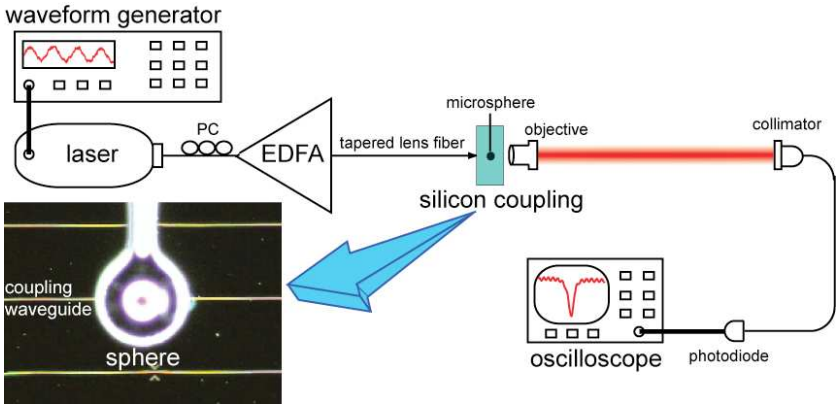

Fig. 4. Experimental setup. Inset shows closeup of microsphere-silicon waveguide coupling region.

5. Results

As we tune over the resonances, transmission dips are observed when coupling to the sphere is achieved, and we measure the width of these transmission dips to obtain the cavity linewidth. We observe a linewidth of 80 MHz in an isolated mode with 7 dB of extinction, as shown in Fig. 5. The Q of the system can then be estimated through the relation,

$$Q = \frac{\omega_0}{\Delta\omega}, \tag{2}$$

where $\Delta\omega$ is the cavity linewidth, and ω_0 is the center frequency. From Eq. 2 we obtain $Q = 2.3\times10^6$, which we believe to be the highest Q achieved in a chalcogenide microresonator by a factor of 10.

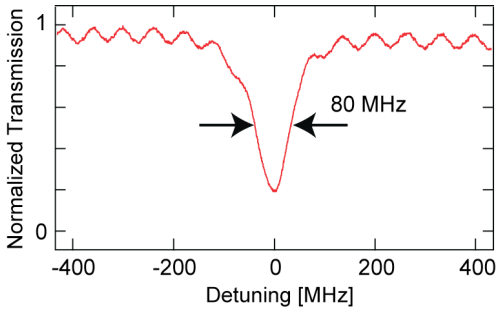

Fig. 5. Isolated As_2Se_3 microsphere mode. The linewidth of the mode is 80 MHz, which corresponds to a Q of 2.3×10^6 at 1550 nm.

#107493 - $15.00 USD Received 11 Feb 2009; revised 23 Mar 2009; accepted 25 Mar 2009; published 30 Mar 2009

In addition to characterizing the Q of the microspheres, we also explore their thermal stability. Comparing As_2Se_3 to silica, we find that thermal instability, stemming from comparatively high linear absorption at 1550 nm and a comparatively low melting temperature, severely limits the viability of As_2Se_3 as a material for NLO oscillation in a microresonator geometry. This instability is manifested in two ways: resonance shifting at low incident powers and melting. We demonstrate the resonance shifts by locating a cavity resonance and increasing the incident power in the waveguide. In Fig. 6(a) we show that with 1 mW of incident power large shifts in the position of the resonance are observed. This shift is due to light being coupled into the sphere mode and heating of the sphere via absorption, which results in a thermal change in the refractive index and a shift of the cavity resonance. If this shift corresponds to the direction of the laser scan, more light will be coupled in, causing further shifting of the resonance. This process will continue until the maximum coupling for the system is reached. At that time, no more light can be coupled into the microsphere, and the laser will scan past the resonance. This leads to the characteristic sharkfin shape seen in Fig. 6(a).

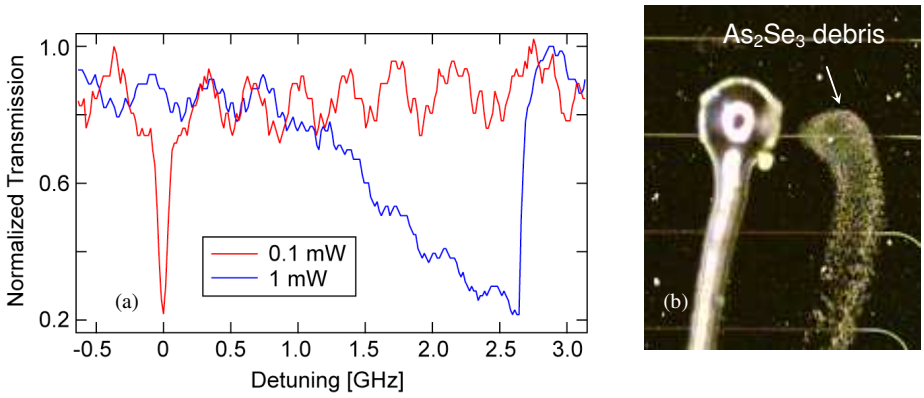

Fig. 6. Temperature instability in As_2Se_3 microspheres. (a) 80-Mhz cavity mode unshifted (red), and shifted by the thermo-optic effect with the characteristic sharkfin shape (blue). (b) Debris ejected from melted microsphere.

At slightly higher incident powers of 2-3 mW, melting occurs, and material may be violently ejected from the sphere. Figure 6(b) shows debris ejected from a microsphere. While thermal resonance shifting can be mitigated with laser locking [37], the melting cannot be solved without cumbersome active cooling. This places a hard limit on useable incident powers and precludes experiments such as broadband cascaded FWM [11] that require incident powers of ~50 mW.

6. Conclusions

We fabricated microspheres with Q's > 2×10^6 and demonstrated efficient coupling to high-Q chalcogenide microspheres via silicon nanowires. We showed that thermal effects limit nonlinear optical performance and found that these thermal effects are present with ≥ 1 mW of incident laser power.

Acknowledgments

This work was funded by the Cornell Center for Nanoscale Systems under NSF grant EEC-0117770. The authors would like to thank P. Londero for useful discussions.

#107493 - $15.00 USD Received 11 Feb 2009; revised 23 Mar 2009; accepted 25 Mar 2009; published 30 Mar 2009